

Flexible Integrated Electrical Cables Based on Biocomposites for Synchronous Energy Transmission and Storage

Hua Wang, Fengshi Li, Bowen Zhu, Lin Guo,* Yun Yang, Rui Hao, Hong Wang, Yaqing Liu, Wei Wang, Xintong Guo, and Xiaodong Chen*

It becomes increasingly important to develop integrated systems with the aim of achieving maximum functionality for the state-of-the-art electronic devices. Here, a flexible integrated electrical cable is reported by incorporating biomaterials based fiber supercapacitors into a resistor–capacitor circuit. In this unique integrated configuration, the fiber electrodes are alternately wound along the twisted electric wires, which worked not only as scaffolding to support and strengthen the slight electrodes but also as separators to spatially confine them to avoid short circuit. It exhibits excellent electrochemical performance comparable to conventional transition metal compounds based cells, and can especially realize sophisticated applications in synchronous energy transmission and storage, presenting a new member for the integrated energy storage system family.

fast-paced life.^[22] For instance, although millions of miles of electrical cables have been used for providing electrical connections, the electrical energy produced from various physical or chemical sources to be distributed to users still need additional energy storage equipment, which causes unnecessary trouble and high cost. Moreover, people are possibly confronted with the inconvenience of sudden loss of power when using indoor electric appliances, and bothered by carrying heavy portable electronic accessories such as batteries and power cords simultaneously during a trip. Integrating the energy storage devices into appropriate energy transmission circuits should be an effective strategy to solve

1. Introduction

It becomes increasingly difficult for the state-of-the-art electronic devices with a single function to meet the requirements of sophisticated applications.^[1–8] The rational design and fabrication of integrated systems with the aim of achieving maximum functionality at minimized size and weight are being intensively pursued.^[9–20] Among them, the integrated energy storage systems are attracting significant attention due to their wide applications and pivotal roles as power sources for electrical equipment.^[21–26] Recently, some integrated systems of energy storage devices with add-on functional modules, such as solar cells,^[27,28] piezoelectric,^[29–31] and triboelectric nanogenerator,^[32–34] photodetector^[35] as well as memristor,^[36] have been successfully fabricated. Nonetheless, more highly targeted designs of integrated energy storage systems should be urgently explored toward overcoming the real-world challenges being suffered by modern human and further facilitating their

the problem of tiring energy distribution, sudden power off, and further lighten the weight of portable electronics, but current research barely involves the integration of energy storage devices and energy transit system, and these two systems still work independently with each other.^[37,38]

Supercapacitor, a promising class of energy storage device, is appealing because of its high power density, long cycle life time, and high energy efficiency.^[39–54] More importantly, supercapacitor can be easily fabricated in various configurations for ease of compatibility and integration with diversified architectures of electronic devices.^[55–64] From this, it can be expected that the integration of appropriate supercapacitor configuration into proper circuit could achieve synchronous energy storage and energy transmission. Besides the configuration, the exploration of naturally abundant and renewable biomaterials with high energy density for the new-generation green supercapacitors is intensively desired.^[65–69] Thus, considering the issues of both the materials and configuration, constructing an ideal integrated supercapacitor system based on renewable biomaterials for synchronous energy storage and transmission should be of scientific and technological importance due to their additional desirable economic, biocompatible and environmental friendly merits.

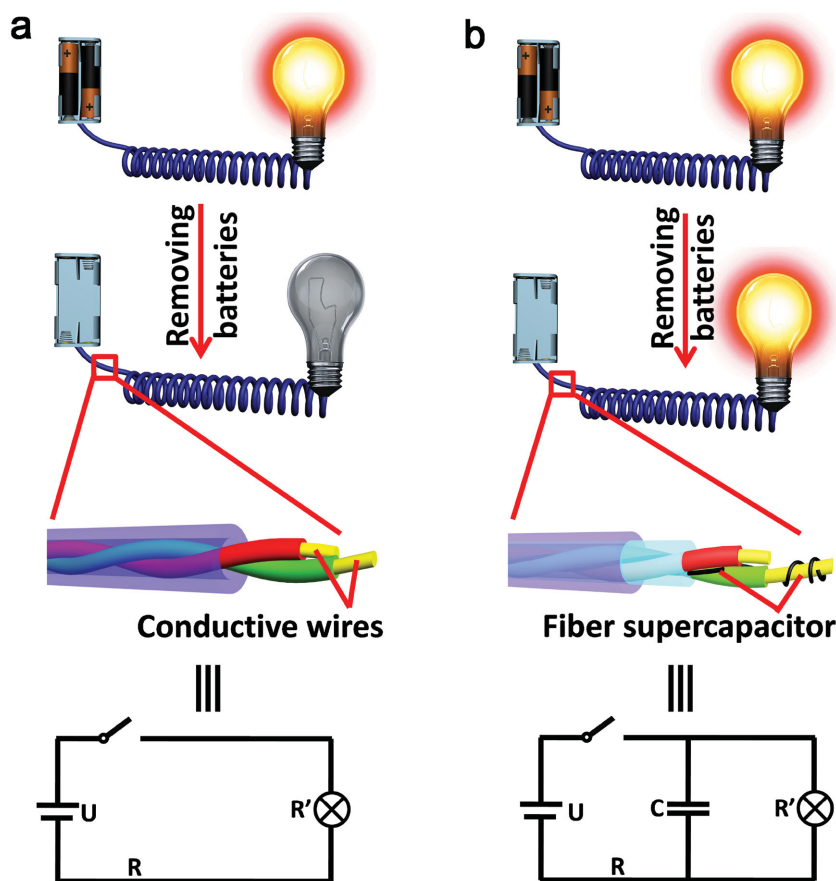
Herein, we report the development of biocomposite-based flexible integrated electrical cable for synchronous energy transmission and storage. In this unique integrated configuration, the fiber electrodes were alternately wound along the twisted electric wires, which worked not only as scaffolding to support and strengthen the slight electrodes but also as separators to spatially confine them to avoid short circuit (**Scheme 1**). Distinct from the conventional electric wires used in a serial

Dr. H. Wang, F. Li, Prof. L. Guo, Y. Yang, R. Hao
School of Chemistry and Environment
Beihang University
Beijing 100191, P. R. China
E-mail: guolin@buaa.edu.cn

Dr. H. Wang, B. Zhu, Dr. H. Wang, Dr. Y. Liu,
Dr. W. Wang, X. Guo, X. Chen
School of Materials Science and Engineering
Nanyang Technological University
Singapore 639798, Singapore
E-mail: chenxd@ntu.edu.sg



DOI: 10.1002/adfm.201600014



Scheme 1. Schematic illustration of the bulbs powered by a) conventional electric wires and b) as-proposed flexible integrated electrical cables.

circuit, the resulting integrated electrical cable along with the external electric appliance constituted a classical parallel resistor–capacitor circuit (RC circuit). Benefited from this rational design, the integrated electrical cable exhibited excellent electrochemical storage capability, and enabled the spontaneously energy storage as a supercapacitor while it simultaneously worked as electron transfer paths just like original electric wires, suggesting the successful integration of energy storage and transmission functionalities in one system. When suddenly shutting off the external power source, the integrated electrical cable could instantly work as substitute to power the electrical appliances spontaneously. Such a characteristic paves up a new approach to solve the problem of tiring energy distribution, indoor sudden power off, and further lighten the weight of portable and wearable electronics. Our work presents a new member with the capability of synchronous energy transmission and storage for the integrated energy storage system family, and demonstrates its great potential for practical applications.

2. Results and Discussion

To achieve the proposed integrated electrical cables, fiber electrodes were first fabricated. Juglone is a renewable biomolecule

naturally derived from the Juglandaceae family, and it has great potential for pseudo-capacitive charge storage owing to the redox centers of its quinone groups (Figure 1a). As organic molecules inherently, juglone-based electrode materials possess beneficial properties of lightweight and ease of processing, but suffer from poor rate capacity due to low conductivity and fast capacity fading owing to its dissolution into electrolyte. Several effectual strategies can be utilized to overcome the mass dissolution and low conductivity issues of organic molecules.^[70–74] In this case, juglone molecules were rationally incorporated into conjugated polypyrrole (PPy) by galvanostatic polymerization. PPy is a conductive polymer, providing sufficient electronic conductivity for the fast redox charge transfer of juglone, while PPy itself possesses good charge storage capabilities due to its reversible surface redox reactions and high conductivity. The as-prepared juglone-doped PPy composite is intrinsically flexible and feasible for electropolymerization deposition on various conductive substrates, suggesting the potential for constructing different supercapacitor configurations. Figure 1b–d are the schematic and optical images of the wire-shaped electrode with juglone/PPy deposited on the conductive carbon fiber, which is flexible enough to intertwine and strong enough to spread. The juglone/PPy composite is a dark film wrapping around the conductive substrate, and the SEM image shows that its surface is a nonuniform facial layer composed of granular clusters compared with the smooth bare carbon fiber (Figure 1e,f). The energy dispersive X-ray diffraction spectroscopy (EDS) mappings (Figure S1, Supporting Information) reveal the composited electrode contains the elements of C, O, and N, which are located uniformly throughout the carbon fiber and overlapped with each other with no impurity phase segregation at microscale or nanoscale, suggesting the juglone molecules have been successfully incorporated into PPy. With the synergistic functions of the conductive PPy and redox electroactive juglone, the as-prepared composite electrode material is expected to exhibit excellent performance for energy storage applications.

As a proof-of-concept, the electrochemical properties of juglone/PPy composite electrode were investigated. Compared with the rectangular current–voltage (CV) curve of bare PPy, the juglone/PPy composite electrode displays one couple of redox wave which should be attributed to the functional quinone group of juglone, suggesting that juglone has been successfully incorporated into the PPy (Figure 1g). It should be noticed that the CV integrated area of bare carbon fiber is very small (Figure S2, Supporting Information), so its contribution to the capacitance of the device is negligible. In addition, the peak separation increases with the scan rate, which shows the quasi reversible electron transfer of juglone (Figure S3a, Supporting Information). Furthermore, the juglone/PPy composite

As a proof-of-concept, the electrochemical properties of juglone/PPy composite electrode were investigated. Compared with the rectangular current–voltage (CV) curve of bare PPy, the juglone/PPy composite electrode displays one couple of redox wave which should be attributed to the functional quinone group of juglone, suggesting that juglone has been successfully incorporated into the PPy (Figure 1g). It should be noticed that the CV integrated area of bare carbon fiber is very small (Figure S2, Supporting Information), so its contribution to the capacitance of the device is negligible. In addition, the peak separation increases with the scan rate, which shows the quasi reversible electron transfer of juglone (Figure S3a, Supporting Information). Furthermore, the juglone/PPy composite

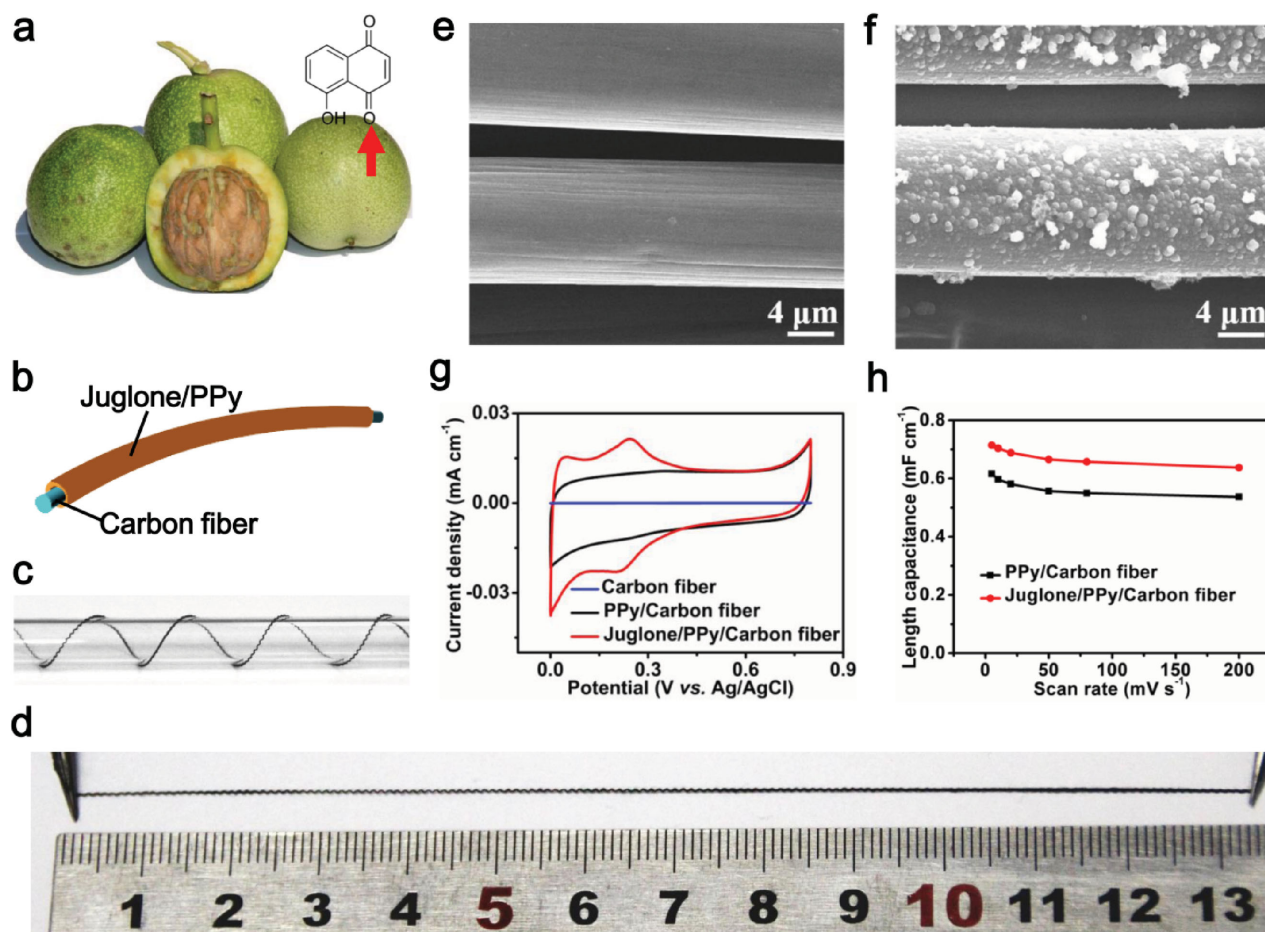


Figure 1. a) Chemical structural formula of Juglone biomolecule which can be derived from the bark of black walnuts. b) Schematic of the as-prepared fiber electrode with juglone/PPy composite deposited on carbon fiber. Optical images of the c) intertwining and d) spreading fiber electrodes. SEM images of e) bare carbon fiber and f) juglone/PPy composite deposited on carbon fiber. g) Cyclic voltammetry curves collected in a three electrode system at a scan rate of 20 mV s^{-1} for bare carbon fiber, PPy/carbon fiber, and juglone/PPy/carbon fiber electrodes with electropolymerization deposition time of 5 min. h) Capacitance comparison of PPy/carbon and juglone/PPy/carbon fiber electrodes at different scan rates (the active length of all fiber electrodes and supercapacitors in this work is 1.8 cm).

shows largely enhanced absolute capacitance compared with that of bare PPy electrode when the scan rate ranges from 5 to 100 mV s^{-1} , and the specific capacitance can be achieved as high as 0.72 mF cm^{-2} at the scan rate of 5 mV s^{-1} , which is higher than 0.61 mF cm^{-2} of bare PPy (Figure 1h). The electrochemical impedance spectroscopy (EIS) revealed that the equivalent series resistances of juglone/PPy composite electrode is only $\approx 7 \Omega$, though a little larger than 5Ω of bare PPy due to the incorporation of insulating juglone, signifying that the low internal resistance would facilitate the charge transfer (Figure S3b, Supporting Information). To achieve higher electrochemical performance, the experimental conditions were optimized by tuning the adding ratio of juglone and pyrrole (Py) as well as the electropolymerization deposition time (Figure S3c,d, Supporting Information). The results showed that the mole ratio of added juglone versus pyrrole at 0.5 and the deposition time of 40 min are most favorable to high capacitance and stability (Figure S4, Supporting Information).

Then, the symmetrical flexible all-solid-state supercapacitor cells based on as-prepared fiber electrodes were fabricated and

characterized. The CV curves are close to rectangular, indicating an excellent capacitance behavior and that the cells are charged and discharged at a pseudoconstant rate over the entire voltammetric cycles (Figure 2a). With the increasing scan rate from 5 to 200 mV s^{-1} , the device exhibited excellent rate capability with 78% retention of the initial capacitance, which is 1.72 mF cm^{-2} calculated from the CV curve (Figure S5a, Supporting Information). To evaluate the flexibility of the resultant fiber supercapacitor, the CV signals were collected under different bending conditions, and no obvious deviation was observed, suggesting that the device is quite stable and suitable for flexible energy storage application (Figure 2b). The capacitances of the flexible juglone-based capacitors were further evaluated by galvanostatic charge/discharge tests at different current densities (Figure S5b, Supporting Information). The linear charge/discharge profiles indicate ideal capacitive characteristics, and the calculated length capacitance at the current density of $5 \mu\text{A cm}^{-2}$ is 1.78 mF cm^{-1} , which is consistent with the capacitance value of 1.72 mF cm^{-2} obtained from CV testing at a scan rate of 5 mV s^{-1} , comparable to that of conventional carbon materials and transition metal

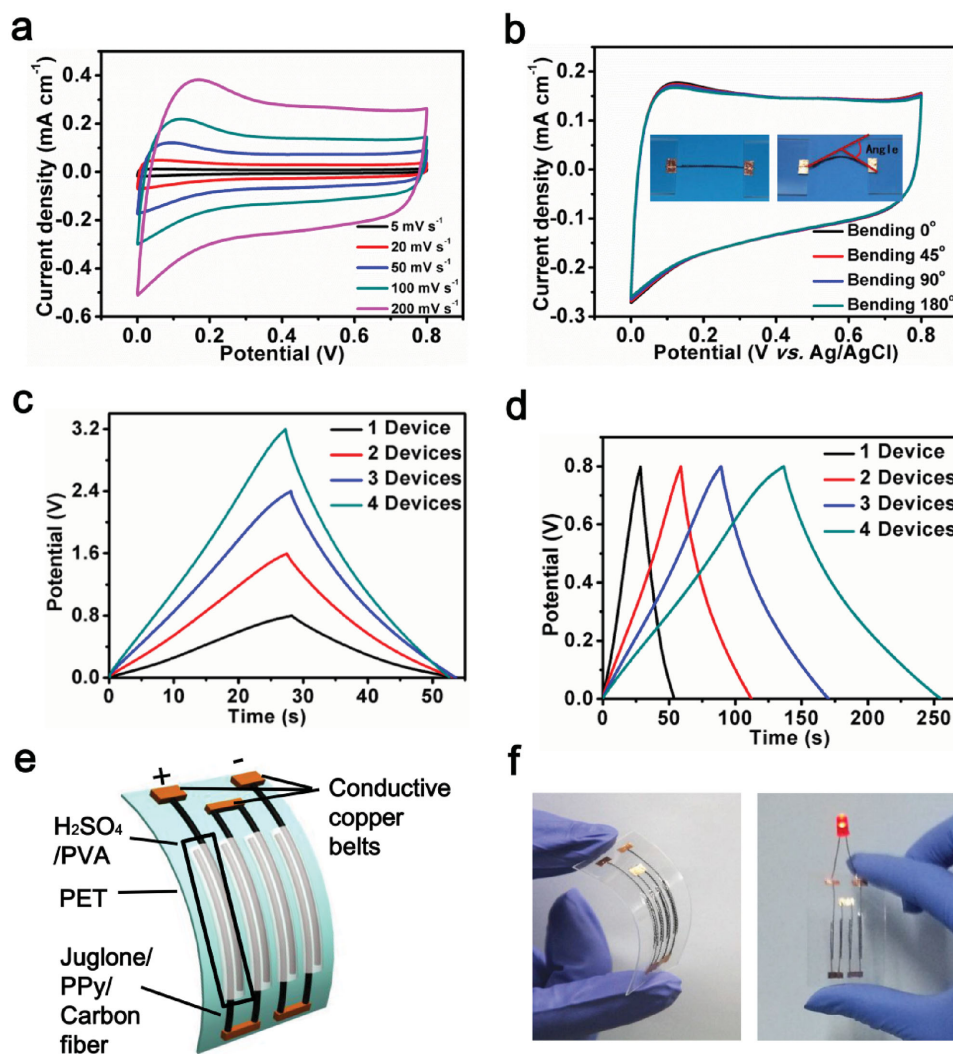


Figure 2. Electrochemical properties of the as-prepared fiber supercapacitor. Cyclic voltammetry curves of the fiber supercapacitor at different a) scan rates and b) bending angles (scan rate is 100 mV s^{-1}). Galvanostatic charge–discharge curves collected at a current density of $12.5 \mu\text{A cm}^{-2}$ of single, two, three or four cells in c) series or d) parallel. e) Schematic and f) the optical images of four tandem cells integrated on a flexible PET substrate.

compounds based supercapacitors reported in literatures.^[75–80] The excellent electrochemical performance should be attributed to the synergistic functions of the conductive PPy and redox electroactive juglone, as well as their unique structural features. The direct deposition of juglone/PPy composite on highly conductive carbon fibers without any binder can effectively facilitate the interfacial charge transfer and transport, and fully exposed fiber electrodes would enable efficient contact with the electrolyte (Figure S5c, Supporting Information). In addition, the charge/discharge cycles were obtained to elucidate the durability performance of the flexible supercapacitors, and it can be seen that the specific capacitance increases gradually in the first 200 cycles due to the self-activation process, while more than 95% of the initial capacitance is retained even after 1000 cycles, suggesting their excellent electrochemical stability (Figure S5d, Supporting Information).

To demonstrate the potential use of these flexible fiber supercapacitors, their serial and parallel connections to manipulate

the operating voltage and current were further studied. In serial connections, the tandem cells exhibit stepwise enhanced operating voltage from 0.8 V for single cell, through 1.6 V for two, and 2.4 for three to 3.2 V for four cells in series with no sacrifice of capacitance (Figure 2c; Figure S5e, Supporting Information). On the other hand, the output currents of two, three or four cells in parallel connections are doubled, tripled or quadrupled, respectively, suggesting correspondingly enhanced capacitance with the same potential window (Figure 2d; Figure S5f, Supporting Information). Such controllable operating voltage and current by simple serial and parallel connections could facilitate their practical applications as energy storage devices. As a proof-of-concept, four cells in serial were integrated on a flexible polyethylene terephthalate (PET) substrate, which can be charged to 3.2 V and then power a light-emitting diode (LED) (Figure 2e,f).

Similar to most of the fiber supercapacitors subjected to practical applications, the as-fabricated cells are also confronted with

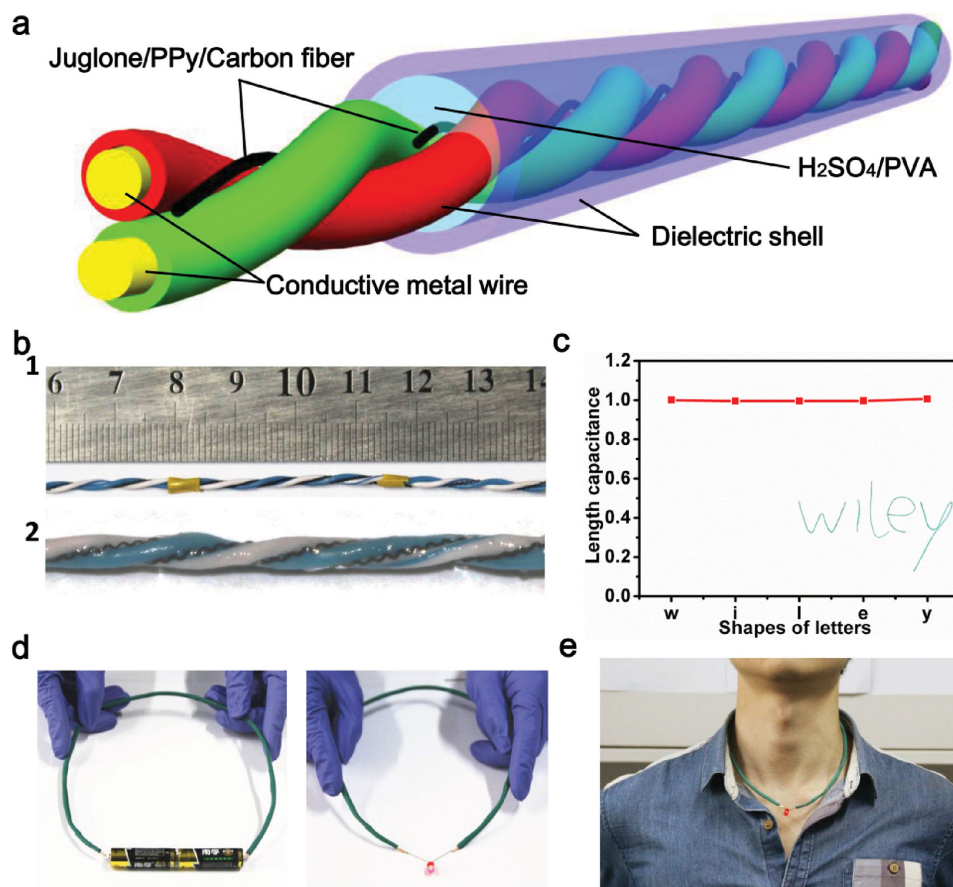


Figure 3. a) Schematic and b) the internal structure of the as-fabricated electric-wire-like supercapacitor; b1) the intertwining electrode fibers on the biaxial twisted electric wires; b2) the partially enlarged view of the electrodes after spreading the gel electrolyte. c) Capacitance retention of the device under bending to form different letters of the word “wiley”. The length capacitance is normalized to 1. d) Demonstration of the electric-wire-like supercapacitor (four cells in series) with the ability for transient energy storage. e) Demonstration of the wearability of the electric-wire-like supercapacitor.

the probability of short circuit and structure fractures, because their wire-shaped electrodes with weak mechanical strength are usually naked and close.^[81] To solve this problem, we develop a simple yet effective approach to achieve strong, spatially confined, and separated fiber electrodes by alternately winding the symmetrical electrode fibers on the biaxial twisted electric wires, which worked as not only scaffold to support and strengthen the slight fibers but also as separators to avoid short circuit (Figure 3a,b). After spreading the gel electrolyte and coating with the polyvinyl chloride (PVC) dielectric cladding material, an electric-wire-like supercapacitor is formed with the potential for practical application. As expected, this electric-wire-like supercapacitor with four cells in series showed excellent electrochemical properties and nearly no capacitance decay when folded to form different letters of word “wiley”, demonstrating its excellent flexibility (Figure 3c). Moreover, it can be quickly charged by two tandem dry cells and then light up a LED, indicating its potential to meet the demand of fast chargeable electronics (Figure 3d). In addition, it shows superior portability and wearability, and can be warped on the neck and powers a red LED looking like a necklace with a ruby (Figure 3e).

Besides the flexible and wearable features, integrating multi-functions in one system is intriguing but challenging. In order to

provide continuously stable power supply despite of occasionally disconnected electricity and further reduce the weight of portable electronics, the intergration of energy transmission and storage modules into one device is urgently needed. To achieve this proposed multifunctional integrated system, constructing a rational circuit is of paramount importance. Inspired by a classical parallel RC circuit with the output voltage equal to the input voltage, it can be expected that a parallel capacitor can store considerable amount of energy while the resistor works. Based on this consideration, further modification of the electric-wire-like supercapacitor was carried out by separately connecting the carbon fibers of the tandem cells to the metal cores on the two side of the electric wire, and then a smart parallel RC circuit was created when an electric appliance was incorporated (Figure S6 and Figure S7, Supporting Information). To demonstrate that the as-prepared integrated flexible electrical cables can concurrently work as energy transmission and energy storage system, dry batteries were used as power source and a LED bulb was connected in a tandem circuit. As shown in Figure 4a, the red LED can first be lighted up by batteries, and then it is interesting to find that the glow can last for several seconds even after removing the batteries, suggesting that the energy has been stored in the integrated flexible electrical cable during the energy transmission process.

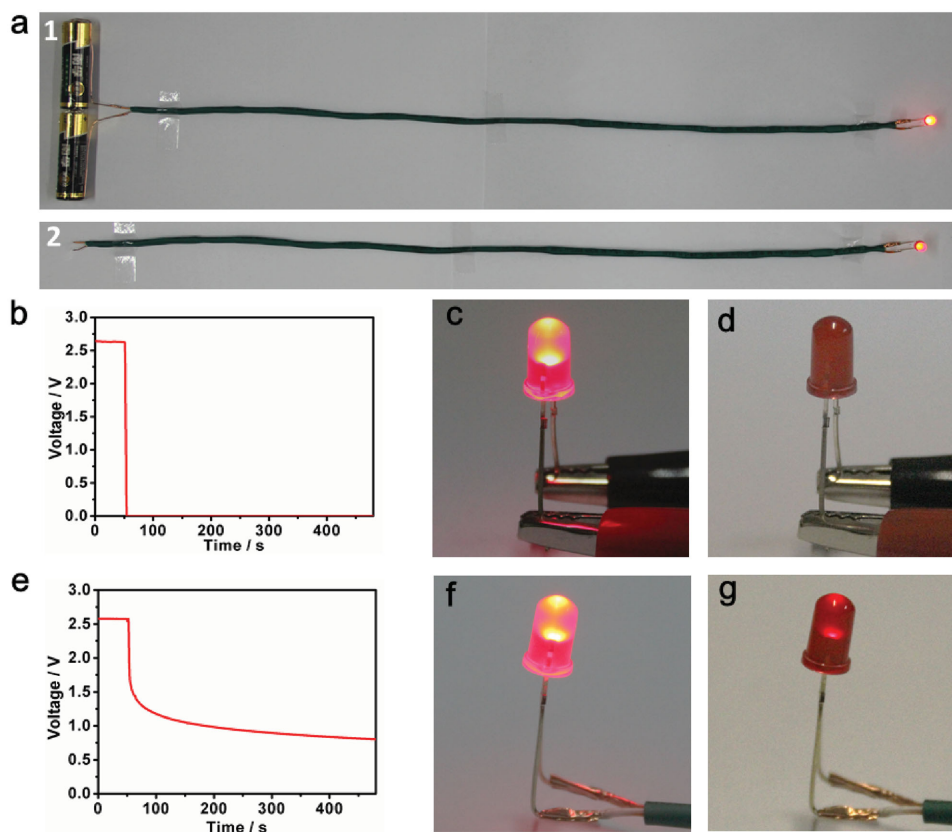


Figure 4. a) Demonstration of the multifunction of the flexible integrated electrical cables for simultaneous energy transmission and storage; a1) an integrated electrical cable was used as the connection to light up a LED; a2) status of the LED after removing the batteries. Variations of the voltage across the bulb versus the time with b) conventional electric wires or e) this integrated electrical cables used as connections in the circuits, which were switched off after 50 s (two tandem dry batteries as the initial power source). The corresponding display of the LED bulbs powered by c) conventional electric wires or f) integrated electrical cables. After shutting off the power, the LED turns off immediately in d) a conventional circuit while the glow can last for more than 5 s in g) an integrated circuit.

To further study the working principle of the integrated electrical cables, the corresponding circuit schematics have been analyzed (Scheme 1). In a conventional circuit with the normal electric wire as connections, the lighted LED was immediately extinguished and the voltage across the bulb steeply dropped to zero after shutting off the power (Figure 5b–d). However, when employing this integrated electrical cable instead of conventional electric wire, a special RC circuit based on electric-wire-like supercapacitor as the capacitor and LED bulb as the resistor was created. More importantly, although the glow can last no more than 10 s, the voltage across the bulb can significantly retain higher than 1.8 V for more than 400 s after switching the power-off, demonstrating that the integrated electrical cable synchronously acted as a conductive wire to transfer electrons and a supercapacitor to store charges (Figure 5e–g). Using the model of RC circuit, the stored electric quantity of the as-fabricated integrated electrical cables can be calculated according to the following equation

$$q = \frac{UCR'}{R'+R} \left\{ 1 - \exp \left[- \left(\frac{1}{R'C} + \frac{1}{RC} \right) t \right] \right\} \quad (1)$$

where U is the electromotive force of the initial power source, C is the capacity of the capacitor, t is the charging time, R' and

R refer to the resistance of the connective electric wires and electrical appliances, respectively. If ignoring the resistance of the connective electric wires, the formula can be simplified to (detailed calculations in the Supporting Information)

$$q = UC \left\{ 1 - \exp \left[- \left(\frac{1}{R'C} \right) t \right] \right\} \quad (2)$$

Thus, the stored electric quantity is related to the C , positively correlated to t , and negatively related to R' . Further enhancing the capacitance of a single fiber supercapacitor or series-parallel connection of multiple cells should be effective strategies to improve the practicability of this integrated flexible electrical cable.

3. Conclusion

In summary, the two fundamental functions of energy transmission and storage were integrated into one flexible electrical cable, by rationally constructing a RC circuit between the fiber supercapacitors and electrical appliances. The all-solid-state symmetrical supercapacitors were fabricated by electropolymerization deposition of renewable juglone

molecules and conductive PPy onto carbon fibers, and showed excellent electrochemical performance comparable to that of conventional carbon materials and transition metal compounds based cells. Integrating the supercapacitor with an electric-wire-based energy transmission system, the resultant device can accomplish the synchronous energy transmission and storage as confirmed by both circuit analysis and display demonstration. Using these integrated cables as electrical connections, the energy distribution and supply applications would be revolutionized, because energy produced by various physical or chemical sources can be distributed to users directly with no need of additional energy storage equipment. Upon sudden power off, the device can immediately work as substitute to power the electrical appliances spontaneously, enabling uninterrupted usage. Additionally, the successful integration of the energy transmission and storage systems provides a new strategy for further lightening the portable electronics via possibly replacing the conventional batteries and electric wires by our integrated multifunctional cables. It is certain that the energy storage capability of as-fabricated integrated electrical cables could be further improved through the series-parallel connection of more cells or replacing the fiber supercapacitors by the wire-shaped batteries with high energy density. Thus, our work presents a new member for the integrated energy storage system family, and it will hold a place in the future next-generation integrated electronics.

4. Experimental Section

Preparation of the Juglone/PPy-Based Fiber Electrodes: The conjugated juglone/PPy composite deposited on the carbon fiber was prepared by galvanostatic polymerization with pyrrole and juglone mixture solution. In preparation of a typical reaction solution, 70 mg of pyrrole, 190 mg of *p*-toluene sulfonic acid, and proper amount of juglone were added to acetonitrile/distilled water (20 mL, 12.5/7.5), and then the mixture was stirred until the solid was completely dissolved. Juglone-free solution was prepared in the same condition without adding juglone molecules for control experiment. After the homogeneous solution being purged with enough N₂, the electropolymerization was performed by a Keithley 4200 semiconductor characterization system at a constant current of 1 mA cm⁻² with suitable time, in the ice bath.

Fabrication of Juglone-Based Flexible Fiber Supercapacitors and Integrated Electrical Cables: The flexible all-solid-state supercapacitors based on as-prepared fiber electrodes with electropolymerization deposition time of 40 min were assembled in a symmetric two-electrode configuration, using the juglone/PPy composite as the active material with a working length of 1.8 cm, and carbon fiber as the current collector, as well as polyvinyl alcohol (PVA)/H₂SO₄ gel as both the electrolyte and the separator. The gel electrolyte was prepared by dissolving 5 mL H₂SO₄ and 5 g PVA powder in 50 mL deionized water at 80 °C with magnetic stirring until the solution became clear.

To fabricate the integrated electrical cable, an electric-wire-like supercapacitor was first prepared by alternately winding the symmetrical electrode fibers on the biaxial twisted electric wires, which worked as scaffold to support and strengthen the slight fibers. After spreading the gel electrolyte and coating with the PVC cladding material, an electric-wire-like supercapacitor was formed. In addition, this electric-wire-like supercapacitor with four cells in series can also be easily fabricated with similar procedures. Further modification of the electric-wire-like supercapacitor was carried out by separately connecting the carbon fibers of the tandem cells with the metal cores on the two sides of the electric wire, and thus a smart flexible electrical cable with the multifunction of simultaneous energy transmission and storage was created.

Characterizations and Electrochemical Tests: The morphologies and EDS elemental mappings of as-prepared electrodes were investigated by the field-emission gun scanning electron microscope (JSM-7600F from JEOL, 5 KV). The electrochemical characterizations of juglone/PPy composite and bare PPy deposited on carbon fiber electrodes were carried out in a standard three-electrode cell containing 1 M H₂SO₄ aqueous electrolyte solutions, using such fibers as working electrodes, a platinum wire as the counter electrode, and a saturated Ag/AgCl electrode as the reference electrode. The flexible fiber supercapacitor cells were measured in a two-electrode configuration. Cyclic voltammetry and galvanostatic charge–discharge measurements were carried out on a supercapacitor test system (Solartron, 1470E) within the voltage range from 0 to 0.8 V. EIS was performed on a CHI 660D electrochemical workstation at an open circuit voltage over the frequency range of 10⁻¹ to 10⁵ Hz with a 10 mV amplitude.

To demonstrate the multifunctionality of the as-prepared flexible integrated electrical cables for synchronous energy transmission and storage, a LED bulb as an electric appliance and two tandem dry batteries as initial power source were connected in the proposed circuits. Variations of the voltage across the bulbs versus the time using conventional electric wires or as-prepared integrated electrical cables as connections were measured by the Keithley 4200 semiconductor characterization system, respectively.

Supporting Information

Supporting Information is available from the Wiley Online Library or from the author

Acknowledgements

H.W. and F.L. contributed equally to this work. This work was supported by the National Key Basic Research Program of China (2014CB931802), National Natural Science Foundation of China (Grant No. 73011701), Fundamental Research Funds for the Central Universities (30428201), and the Singapore MOE Tier 2 (MOE2015-T2-1-110).

Received: January 2, 2016

Published online: February 23, 2016

- [1] A. Vlad, N. Singh, C. Galande, P. M. Ajayan, *Adv. Energy Mater.* **2015**, *5*, 1402115.
- [2] T. Miyasaka, T. N. Murakami, *Appl. Phys. Lett.* **2004**, *85*, 3932.
- [3] J. Xu, G. Shen, *Nano Energy* **2015**, *13*, 131.
- [4] M. F. El-Kady, M. Ihns, M. P. Li, J. Y. Hwang, M. F. Mousavi, L. Chaney, A. T. Lech, R. B. Kaner, *Proc. Natl. Acad. Sci.* **2015**, *112*, 4233.
- [5] X. F. Wang, B. Liu, Q. F. Wang, W. F. Song, X. J. Hou, D. Chen, Y. B. Cheng, G. Shen, *Adv. Mater.* **2013**, *25*, 1479.
- [6] C. T. Chien, P. Hiralal, D. Y. Wang, I. S. Huang, C. C. Chen, C. W. Chen, G. A. J. Amaratunga, *Small* **2015**, *11*, 2929.
- [7] L. Peng, L. F. Hu, X. S. Fang, *Adv. Funct. Mater.* **2014**, *24*, 2591.
- [8] S. Jung, J. Lee, T. Hyeon, M. Lee, D.-H. Kim, *Adv. Mater.* **2014**, *26*, 6329.
- [9] J. Wang, L. Zhang, L. Yu, Z. Jiao, H. Xie, X. W. Lou, X. W. Sun, *Nat. Commun.* **2014**, *5*, 4921.
- [10] U. N. Maiti, J. Lim, K. E. Lee, W. J. Lee, S. O. Kim, *Adv. Mater.* **2014**, *26*, 615.
- [11] P. Du, X. Hu, C. Yi, H. C. Liu, P. Liu, H.-L. Zhang, X. Gong, *Adv. Funct. Mater.* **2015**, *25*, 2420.
- [12] L. Nyholm, G. Nystrom, A. Mihranyan, M. Stromme, *Adv. Mater.* **2011**, *23*, 3751.

- [13] H. Sun, X. You, J. Deng, X. Chen, Z. Yang, P. Chen, X. Fang, H. Peng, *Angew. Chem., Int. Ed.* **2014**, *53*, 6664.
- [14] D. Yu, Q. Qian, L. Wei, W. Jiang, K. Goh, J. Wei, J. Zhang, Y. Chen, *Chem. Soc. Rev.* **2015**, *44*, 647.
- [15] J. J. Yoo, K. Balakrishnan, J. S. Huang, V. Meunier, B. G. Sumpter, A. Srivastava, M. Conway, A. L. M. Reddy, J. Yu, R. Vajtai, P. M. Ajayan, *Nano Lett.* **2011**, *11*, 1423.
- [16] N. Li, Y. R. Wang, D. M. Tang, H. S. Zhou, *Angew. Chem., Int. Ed.* **2015**, *54*, 9271.
- [17] L. Li, S. M. Chen, X. B. Wang, Y. Bando, D. Golberg, *Energy Environ. Sci.* **2012**, *5*, 6040.
- [18] Y. N. Meng, Y. Zhao, C. G. Hu, H. H. Cheng, Y. Hu, Z. P. Zhang, G. Q. Shi, L. T. Qu, *Adv. Mater.* **2013**, *25*, 2326.
- [19] K. Y. Xie, B. Q. Wei, *Adv. Mater.* **2014**, *26*, 3592.
- [20] N. S. Liu, W. Z. Ma, J. Y. Tao, X. H. Zhang, J. Su, L. Y. Li, C. X. Yang, Y. H. Gao, D. Golberg, Y. Bando, *Adv. Mater.* **2013**, *25*, 4925.
- [21] X. Chen, H. Lin, J. Deng, Y. Zhang, X. Sun, P. Chen, X. Fang, Z. Zhang, G. Guan, H. Peng, *Adv. Mater.* **2014**, *26*, 8126.
- [22] X. Wang, X. Lu, B. Liu, D. Chen, Y. Tong, G. Shen, *Adv. Mater.* **2014**, *26*, 4763.
- [23] J. Xu, H. Wu, L. Lu, S.-F. Leung, D. Chen, X. Chen, Z. Fan, G. Shen, D. Li, *Adv. Funct. Mater.* **2014**, *24*, 1840.
- [24] M. Yu, Y. Han, X. Cheng, L. Hu, Y. Zeng, M. Chen, F. Cheng, X. Lu, Y. Tong, *Adv. Mater.* **2015**, *27*, 3085.
- [25] D. S. Yu, Q. H. Qian, L. Wei, W. C. Jiang, K. L. Goh, J. Wei, J. Zhang, Y. Chen, *Chem. Soc. Rev.* **2015**, *44*, 647.
- [26] X. L. Chen, H. J. Lin, P. N. Chen, G. Z. Guan, J. Deng, H. S. Peng, *Adv. Mater.* **2014**, *26*, 4444.
- [27] T. Chen, L. Qiu, Z. Yang, Z. Cai, J. Ren, H. Li, H. Lin, X. Sun, H. Peng, *Angew. Chem., Int. Ed.* **2012**, *51*, 11977.
- [28] X. Zhang, X. Z. Huang, C. S. Li, H. R. Jiang, *Adv. Mater.* **2013**, *25*, 4093.
- [29] X. Y. Xue, S. H. Wang, W. X. Guo, Y. Zhang, Z. L. Wang, *Nano Lett.* **2012**, *12*, 5048.
- [30] Y. C. Mao, P. Zhao, G. McConohy, H. Yang, Y. X. Tong, X. D. Wang, *Adv. Energy Mater.* **2014**, *4*, 1301624.
- [31] A. Ramadoss, B. Saravanakumar, S. W. Lee, Y. S. Kim, S. J. Kim, Z. L. Wang, *ACS Nano* **2015**, *9*, 4337.
- [32] J. Wang, X. Li, Y. Zi, S. Wang, Z. Li, L. Zheng, F. Yi, S. Li, Z. L. Wang, *Adv. Mater.* **2015**, *27*, 4830.
- [33] P. Bai, G. Zhu, Z. H. Lin, Q. S. Jing, J. Chen, G. Zhang, J. Ma, Z. L. Wang, *ACS Nano* **2013**, *7*, 3713.
- [34] S. H. Wang, Z. H. Lin, S. M. Niu, L. Lin, Y. N. Xie, K. C. Pradel, Z. L. Wang, *ACS Nano* **2013**, *7*, 11263.
- [35] X. Wang, B. Liu, R. Liu, Q. Wang, X. Hou, D. Chen, R. Wang, G. Shen, *Angew. Chem., Int. Ed.* **2014**, *53*, 1849.
- [36] B. Liu, B. Liu, X. Wang, X. Wu, W. Zhao, Z. Xu, D. Chen, G. Shen, *Adv. Mater.* **2014**, *26*, 4999.
- [37] Z. B. Yang, J. Deng, H. Sun, J. Ren, S. W. Pan, H. S. Peng, *Adv. Mater.* **2014**, *26*, 7038.
- [38] Z. Yu, J. Thomas, *Adv. Mater.* **2014**, *26*, 4279.
- [39] M. Winter, R. J. Brodd, *Chem. Rev.* **2004**, *104*, 4245.
- [40] Y. N. Meng, K. Wang, Y. J. Zhang, Z. X. Wei, *Adv. Mater.* **2013**, *25*, 6985.
- [41] Z. H. Wen, X. C. Wang, S. Mao, Z. Bo, H. Kim, S. M. Cui, G. H. Lu, X. L. Feng, J. H. Chen, *Adv. Mater.* **2012**, *24*, 5610.
- [42] H. Yang, Z. Y. Liu, B. K. Chandran, J. Y. Deng, J. C. Yu, D. P. Qi, W. D. Li, Y. X. Tang, C. G. Zhang, X. D. Chen, *Adv. Mater.* **2015**, *27*, 5593.
- [43] F. Béguin, V. Presser, A. Balducci, E. Frackowiak, *Adv. Mater.* **2014**, *26*, 2219.
- [44] L.-F. Chen, Z.-H. Huang, H.-W. Liang, Q.-F. Guan, S.-H. Yu, *Adv. Mater.* **2013**, *25*, 4746.
- [45] S. Gao, Y. Sun, F. Lei, L. Liang, J. Liu, W. Bi, B. Pan, Y. Xie, *Angew. Chem., Int. Ed.* **2014**, *53*, 12789.
- [46] D. Vonlanthen, P. Lazarev, K. A. See, F. Wudl, A. J. Heeger, *Adv. Mater.* **2014**, *26*, 5095.
- [47] G. Sun, X. Zhang, R. Lin, J. Yang, H. Zhang, P. Chen, *Angew. Chem., Int. Ed.* **2015**, *54*, 4651.
- [48] H. Tang, J. Wang, H. Yin, H. Zhao, D. Wang, Z. Tang, *Adv. Mater.* **2015**, *27*, 1117.
- [49] B. L. Ellis, P. Knauth, T. Djenizian, *Adv. Mater.* **2014**, *26*, 3368.
- [50] W. Wang, W. Liu, Y. Zeng, Y. Han, M. Yu, X. Lu, Y. Tong, *Adv. Mater.* **2015**, *27*, 3572.
- [51] S. Chabi, C. Peng, D. Hu, Y. Zhu, *Adv. Mater.* **2014**, *26*, 2440.
- [52] X. Yu, B. Lu, Z. Xu, *Adv. Mater.* **2014**, *26*, 1044.
- [53] H. Wang, B. Zhu, W. Jiang, Y. Yang, W. R. Leow, H. Wang, X. Chen, *Adv. Mater.* **2014**, *26*, 3638.
- [54] J. R. Miller, P. Simon, *Science* **2008**, *321*, 651.
- [55] N. Liu, W. Ma, J. Tao, X. Zhang, J. Su, L. Li, C. Yang, Y. Gao, D. Golberg, Y. Bando, *Adv. Mater.* **2013**, *25*, 4925.
- [56] T. Chen, R. Hao, H. Peng, L. Dai, *Angew. Chem., Int. Ed.* **2015**, *54*, 618.
- [57] C. Choi, J. A. Lee, A. Y. Choi, Y. T. Kim, X. Lepró, M. D. Lima, R. H. Baughman, S. J. Kim, *Adv. Mater.* **2014**, *26*, 2059.
- [58] Y. Wang, Y. Xia, *Adv. Mater.* **2013**, *25*, 5336.
- [59] M. Yu, Y. Zhang, Y. Zeng, M. S. Balogun, K. Mai, Z. Zhang, X. Lu, Y. Tong, *Adv. Mater.* **2014**, *26*, 4724.
- [60] S. K. Kim, H. J. Koo, A. Lee, P. V. Braun, *Adv. Mater.* **2014**, *26*, 5108.
- [61] L. L. Liu, Z. Q. Niu, L. Zhang, W. Y. Zhou, X. D. Chen, S. S. Xie, *Adv. Mater.* **2014**, *26*, 4855.
- [62] S. W. Pan, H. J. Lin, J. Deng, P. N. Chen, X. L. Chen, Z. B. Yang, H. S. Peng, *Adv. Energy Mater.* **2014**, *4*, 1401438.
- [63] D. P. Qi, Z. Y. Liu, Y. Liu, W. R. Leow, B. W. Zhu, H. Yang, J. C. Yu, W. Wang, H. Wang, S. Y. Yin, X. D. Chen, *Adv. Mater.* **2015**, *27*, 5559.
- [64] Z. Q. Niu, L. Zhang, L. L. Liu, B. W. Zhu, H. B. Dong, X. D. Chen, *Adv. Mater.* **2013**, *25*, 4035.
- [65] G. Milczarek, O. Inganäs, *Science* **2012**, *335*, 1468.
- [66] M. Armand, J. M. Tarascon, *Nature* **2008**, *451*, 652.
- [67] O. Inganäs, S. Admassie, *Adv. Mater.* **2014**, *26*, 830.
- [68] D. H. Nagaraju, T. Rebis, R. Gabrielsson, A. Elfving, G. Milczarek, O. Inganäs, *Adv. Energy Mater.* **2014**, *4*, 1300443.
- [69] H. Wang, P. Hu, J. Yang, G. Gong, L. Guo, X. Chen, *Adv. Mater.* **2015**, *27*, 2348.
- [70] B. Genorio, K. Pirnat, R. Cerc-Korošec, R. Dominko, M. Gaberscek, *Angew. Chem., Int. Ed.* **2010**, *49*, 7222.
- [71] Y. Hanyu, T. Sugimoto, Y. Ganbe, A. Masuda, I. Honma, *J. Electrochem. Soc.* **2013**, *161*, A6.
- [72] Q. Su, S. Pang, V. Aljani, C. Li, X. Feng, K. Müllen, *Adv. Mater.* **2009**, *21*, 3191.
- [73] Y. Morita, S. Nishida, T. Murata, M. Moriguchi, A. Ueda, M. Satoh, K. Arifuku, K. Sato, T. Takui, *Nat. Mater.* **2011**, *10*, 947.
- [74] A. Shimizu, H. Kuramoto, Y. Tsujii, T. Nokami, Y. Inatomi, N. Hojo, H. Suzuki, J.-I. Yoshida, *J. Power Sources* **2014**, *260*, 211.
- [75] D. H. Zhang, M. H. Miao, H. T. Niu, Z. X. Wei, *ACS Nano* **2014**, *8*, 4571.
- [76] J. A. Lee, M. K. Shin, S. H. Kim, H. U. Cho, G. M. Spinks, G. G. Wallace, M. D. Lima, X. Lepro, M. E. Kozlov, R. H. Baughman, S. J. Kim, *Nat. Commun.* **2013**, *4*, 1970.
- [77] J. Ren, L. Li, C. Chen, X. L. Chen, Z. B. Cai, L. B. Qiu, Y. G. Wang, X. R. Zhu, H. S. Peng, *Adv. Mater.* **2013**, *25*, 1155.
- [78] V. T. Le, H. Kim, A. Ghosh, J. Kim, J. Chang, Q. A. Vu, D. T. Pham, J. H. Lee, S. W. Kim, Y. H. Lee, *ACS Nano* **2013**, *7*, 5940.
- [79] J. Bae, M. K. Song, Y. J. Park, J. M. Kim, M. L. Liu, Z. L. Wang, *Angew. Chem., Int. Ed.* **2011**, *50*, 1683.
- [80] Y. Huang, H. Hu, Y. Huang, M. S. Zhu, W. J. Meng, C. Liu, Z. X. Pei, C. L. Hao, Z. K. Wang, C. Y. Zhi, *ACS Nano* **2015**, *9*, 4766.
- [81] L. Kou, T. Huang, B. Zheng, Y. Han, X. Zhao, K. Gopalsamy, H. Sun, C. Gao, *Nat. Commun.* **2014**, *5*, 3754.